PAPER • OPEN ACCESS

Nuclear magnetic resonance investigation of superconducting and normal state Nb_3Sn

View the article online for updates and enhancements.

Nuclear magnetic resonance investigation of superconducting and normal state Nb$_3$Sn

Gan Zhai[1],[*] , William P Halperin[1],[*] , Arneil P Reyes[2], Sam Posen[3], Zuhawn Sung[3] , Chiara Tarantini[2] , Michael D Brown[4] and David C Larbalestier[2]

[1] Department of Physics and Astronomy, Northwestern University, Evanston, IL 60208, United States of America
[2] National High Magnetic Field Laboratory, Tallahassee, FL 32310, United States of America
[3] Fermi National Accelerator Laboratory, Batavia, IL 60510, United States of America
[4] Bruker OST, Carteret, NJ 07008, United States of America

E-mail: ganzhai2025@u.northwestern.edu and w-halperin@northwestern.edu

Abstract

The superconductor Nb$_3$Sn has important applications for construction of very high-field superconducting magnets. In this work we investigate its microscopic electronic structure with ^{93}Nb nuclear magnetic resonance (NMR). The high-quality Nb$_3$Sn powder sample was studied in both 3.2 T and 7 T magnetic fields in the temperature range from 4 K to 300 K. From measurement of the spectrum and its theoretical analysis, we find evidence for anisotropy despite its cubic crystal structure. Magnetic alignment of the powder grains in the superconducting state was also observed. The Knight shift and spin-lattice relaxation rate, T_1^{-1}, were measured and the latter compared with BCS theory for the energy gap $\Delta(0) = 2.7 \pm 0.3\,k_{\rm B}T_{\rm c}$ at 3.2 T and $\Delta(0) = 2.33 \pm 0.07\,k_{\rm B}T_{\rm c}$ at 7 T, indicating suppression of the order parameter by magnetic field.

Keywords: nuclear magnetic resonance, superconductivity, Nb$_3$Sn, spin lattice relaxation, superconducting energy gap

1. Introduction

Nb$_3$Sn is widely used for producing superconducting magnet wires. Its high critical temperature $T_{\rm c}(\sim 18\,{\rm K})$ and high critical field $H_{\rm c2}(\sim 30\,{\rm T})$ [1] make it possible to generate very high magnetic fields at liquid helium temperatures, such as for NMR high resolution magnets operating in the 1 GHz range and hybrid magnets at the National High Magnetic Field Laboratory reaching 45 T. Significant amounts of Nb$_3$Sn, ~ 875 tons, have been used for the ITER tokamak magnets [2]. Recent research shows that this material can also be used for superconducting radio frequency (SRF) cavities [3].

Nuclear magnetic resonance (NMR) has traditionally played a key role in the investigation of superconducting materials both in normal and superconducting states, in low and high magnetic fields and at low temperatures [4]. The electronic coupling to the nuclear spin provides direct information from NMR about the density of electronic states, the amplitude of the superconducting order parameter, and superconducting vortex structure [5]. However, despite important applications for Nb$_3$Sn, the electronic structure properties of this material have not been extensively studied with NMR. An early effort using ^{93}Nb NMR in 1973 [6] was incomplete, notably in the

superconducting state. We have overcome those earlier limitations and present our work here.

2. Sample preparation and characterization

The high-quality powder sample, 20 mg, was produced in the Applied superconductivity Center of the National High Magnetic Field Laboratory following a process of high-energy ball milling, initial cold isostatic press densification, and final hot isostatic press reaction and densification at 1800 °C [1]. Our sample was made from 27% Sn and 73% Nb expressed in atomic percent; therefore, it is slightly Sn-rich (T_c = 17.2 K, H_{c2} = 28.5 T at 1.2 K). According to x-ray characterization (XRD) it has a typical cubic A15 crystal structure, shown in figure 1. For this composition and processing there is no evidence of tetragonal structure. The Sn atoms occupy the corners and the body-centered positions of a unit cell, while the Nb atoms lie on three orthogonal chains on each face of the cube.

3. Experiment

The NMR experiments were performed at Northwestern University in a magnetic field of 14 T, and at the National High Magnetic Field Laboratory with a magnetic field of 3.2 T and 7 T.

Given that the Nb nucleus has a spin I = 9/2, there are strong quadrupolar components to a broad spectrum. For a random powder, this results in a short signal decay time, less than the dead time of the spectrometer. Therefore, instead of a single free induction decay, we used a Hahn echo (90°–180° tip angle technique) for all NMR measurements. We swept the frequency over a wide range in order to capture the full spectrum.

The superconducting transition temperature T_c is 14.43 K at 7 T and 16.06 K at 3.2 T identified from heat capacity measurement and consistent with *in situ* detuning of the NMR coil at onset of superconductivity. The temperature dependence of the susceptibility was measured with a SQUID demonstrating absence of paramagnetic impurities.

4. Results

4.1. Spectrum

The expected nine component spectrum of ^{93}Nb was measured at 80 K in a field of 7 T, as shown in figure 2(a) for what we have determined from spectrum analysis is a randomly oriented powder. This can be compared with spectra at different temperatures from the oriented sample shown in figure 2(b). The difference between the two cases (a) and (b) can be attributed to a field-temperature cycle producing preferential magnetic alignment below T_c. The shape of the spectra in figure 2(a) was analyzed using the theory given by Carter *et al* [7]. The line shape depends on an anisotropic Knight
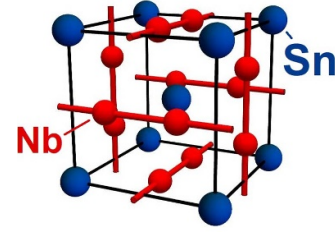
Figure 1. Crystal structure of Nb$_3$Sn.

shift and the nuclear quadrupole coupling to the local electric field gradient, principally from near neighbors. It depends on the relative orientation of the crystal axes with respect to the magnetic field. We speculate, that ball milling Nb$_3$Sn fractures the bulk polycrystalline material at crystal grain boundaries since the surfeit of Sn segregates at the grain boundary [1]. Alignment resulting from magnetic anisotropy will be discussed later. The anisotropic Knight shift can be expressed quantitatively by separating the Knight shift into isotropic and axial components, K_{iso} and K_{ax}. We can then determine the central transition frequency $\nu_0 = \nu_R(1 + K_{iso})$ and its anisotropic factor $a = K_{ax}/(1 + K_{iso})$.

The nuclear quadrupole interaction depends on the nuclear quadrupole moment Q and the local electric field gradient **q** (EFG) . The effect of the quadrupole interaction on the NMR frequency is expressed in terms of the quadrupole frequency, defined as $\nu_Q = 3e^2qQ/2I(2I-1)h$ and is a measure of the separation in frequencies of the spectral components.

The resonance frequency of a nucleus with spin $I \neq 1/2$ in a single crystal, correct to second order in perturbation theory, is:

$$
\begin{aligned}
\nu(m \leftrightarrow m-1) = \nu_0 &+ \left(3\mu^2 - 1\right)\left[a + 1/2\nu_Q(m-1/2)\right] \\
&+ 1/32\left(\left(\nu_Q^2\right)/\nu_0\right)\left(1-\mu^2\right) \\
&\times \left\{\left[102m(m-1) - 18I(I+1) + 39\right]\mu^2 \right.\\
&\left. - \left[6m(m-1) - 2I(I+1) + 3\right]\right\}.
\end{aligned}
$$
(1)

In this expression, $\mu \equiv \cos\theta$, where θ is the angle between the EFG and the external magnetic field. In Nb$_3$Sn, the EFG for the Nb nucleus is parallel to the Nb chains. In a randomly oriented powder sample, the direction of the EFG is equally distributed in space, producing a uniform distribution of μ from −1 to 1. With this distribution, we can simulate the spectrum by convolving the orientational frequency distribution function with a shape function, taken as a Gaussian distribution with a standard deviation $\Delta\nu_0$ [6]. Note that $\Delta\nu_0$ includes both homogeneous and inhomogeneous broadening. The homogeneous component is determined by the intrinsic T_2, while the inhomogeneous component is dominated by the orientation distribution of the EFG. Hence in the simulation, $\Delta\nu_0$ is larger for outer satellites, with a ratio of 1:2:4:8:16, extending from the central transition to the outermost satellites. From the
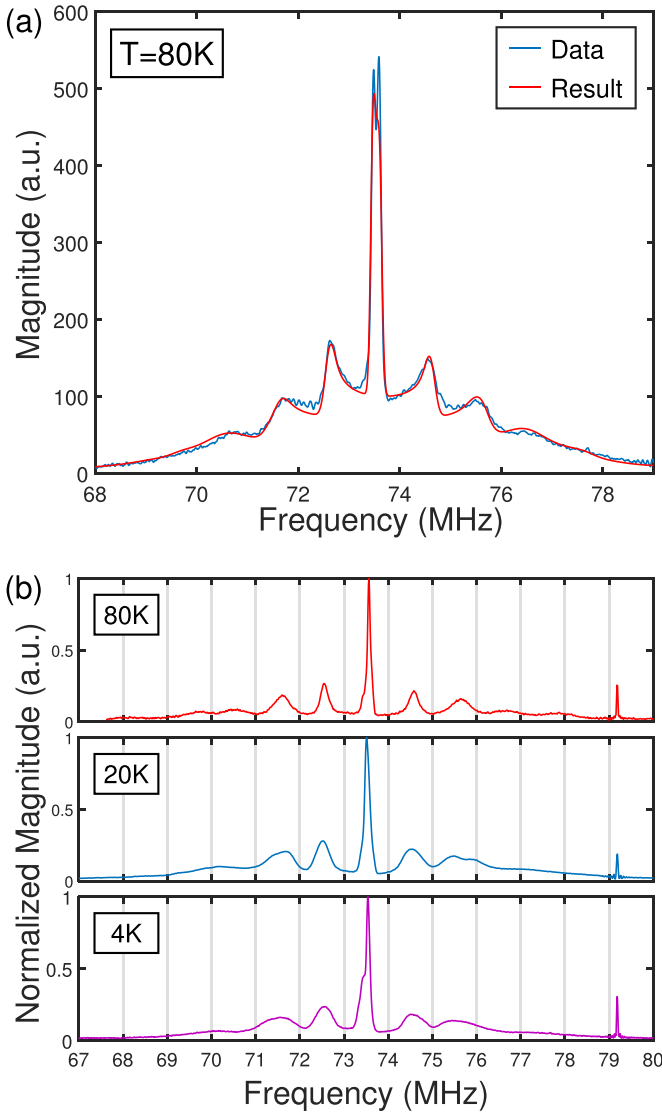
Figure 2. Nb$_3$Sn Spectra at 7 T. (a) ^{93}Nb spectrum at 80 K field cooled. The red line is a fit with the theory, Carter *et al* [7]. (b) ^{93}Nb spectra at 4 K, 20 K and 80 K after cooling to 1.5 K in low field and then ramping to 7 T. The small peak on the right side is the ^{63}Cu signal from the NMR coil. The quadrupolar broadening of the satellites is noticeably decreased, indicating an alignment effect in the powder sample. The dome-like background in (a) results from a significant overlap of the satellites in the random powder.

simulation, the anisotropic Knight shift was determined to be $K_{\mathrm{ax}} = 0.5\%$.

As mentioned above, we found that cycling the field at low temperature in the superconducting state resulted in some degree of alignment. This is reflected in the spectra shown in figure 2(b), clearly distinct from that in figure 2(a). The three spectra in figure 2(b) deviate from a typical random powder spectrum, which has a dome-like background corresponding to a broad distribution of orientations of electric field gradients. The line shape of the satellites are consistent with the distribution of μ to be enhanced at either the limits $\mu = 0$ or $\mu = 1$, indicating respectively that the powder grains are more, or less, aligned with the external field. This argument requires

that a significant fraction of the powder grains have a high degree of crystallinity, as well as anisotropy in the magnetization. figure 2(b) shows that when ramping up the temperature, the line shape is preserved from 4 K to 80 K, meaning that this ordering is stable and not restricted to the superconducting state. A detailed study of the alignment phenomenon will be undertaken in future work.

4.2. Normal state measurements

The total frequency shift, K, in the normal state was measured at the central transition from room temperature to 20 K. K has two components, the spin component K_{s}, also known as the Knight shift, and the orbital and diamagnetic component K_{o}, given in equation (2). The latter, K_{o}, is temperature independent and can be obtained from the zero temperature limit of the total shift K, since the spin component K_{s} is fully eliminated due to the formation of Cooper pairs in the superconducting state. In this case we have $K_{\mathrm{o}} = 0.8835\%$ relative to the Larmor frequency. Then the Knight Shift K_{s} can be extracted from the total shift and plotted in figure 3(a)

$$K = K_{\mathrm{s}} + K_{\mathrm{o}}. \tag{2}$$

The temperature dependence of the Knight shift can be attributed to core polarization of the Nb atomic orbitals. The decrease of the Knight shift with decreasing temperature indicates that the core polarization contribution to the shift is enhanced at lower temperatures. The dependence of the Knight shift and the spin lattice relaxation rate T_1^{-1} are given in equations (3) and (4), the latter is known as the Korringa relation, expressed in terms of the density of states, $\rho(E_{\mathrm{F}})$, at the Fermi surface compared to the free electron case, $\rho_0(E_{\mathrm{F}})$.

$$K_{\mathrm{s}} = \frac{8\pi}{3}\mu_0\mu_{\mathrm{B}}{}^2 \langle |u_k(0)^2| \rangle_{E_{\mathrm{F}}} \rho(E_{\mathrm{F}}) \tag{3}$$

$$T_1 T K_{\mathrm{s}}^2 = \frac{\hbar}{4\pi k_{\mathrm{B}}} \frac{\gamma_e^2}{\gamma_n^2} \left[\frac{\chi_e^s}{\chi_0^s} \frac{\rho_0(E_{\mathrm{F}})}{\rho(E_{\mathrm{F}})} \right]^2. \tag{4}$$

The spin-lattice relaxation rate was measured at the central transition, and the Korringa relation is plotted in figure 3(b). The measurements were performed with a saturation recovery pulse sequence (90°–90°–180°), using a Hahn echo for detection as was discussed above. Given that Nb is a spin 9/2 nuclei, the T_1 was obtained from a stretched master-equation fit allowing for the relaxation of the quadrupolar satellites, equation (5), for the recovery of the NMR signal M with $\beta \approx 0.9$

$$M = M_0 - M_0 \left[\frac{1}{165}\exp\left(-t/T_1\right)^\beta + \frac{24}{715}\exp\left(-6t/T_1\right)^\beta \right.$$
$$+ \frac{6}{65}\exp\left(-15t/T_1\right)^\beta + \frac{1568}{7293}\exp\left(-28t/T_1\right)^\beta$$
$$\left. + \frac{7938}{12\,155}\exp\left(-45t/T_1\right)^\beta \right]. \tag{5}$$
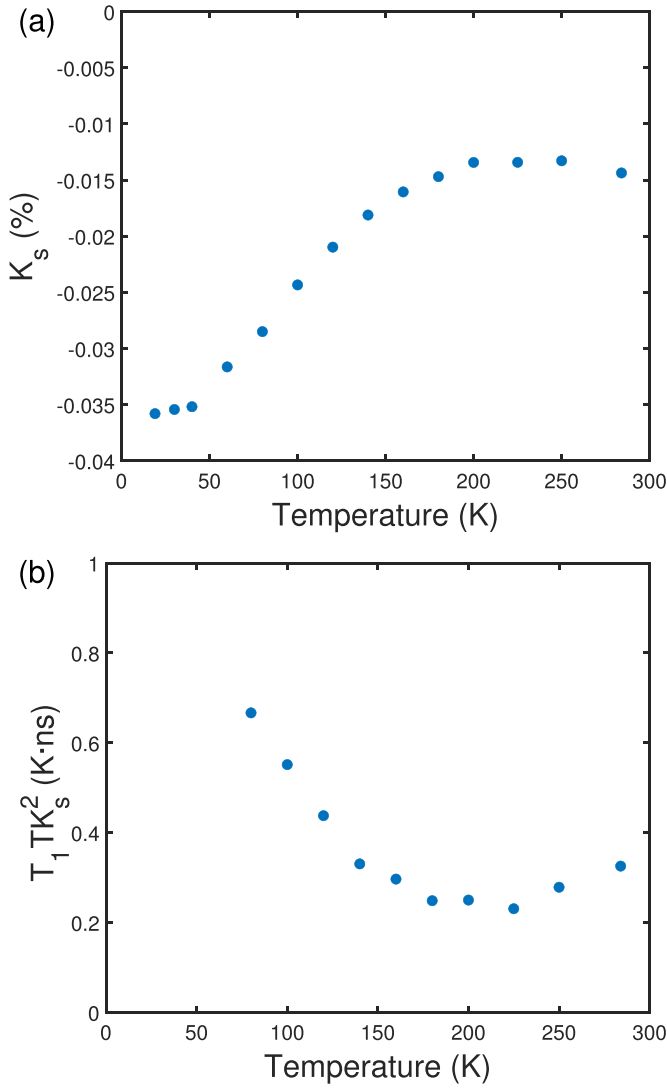
Figure 3. Temperature dependence of the ^{93}Nb Knight shift, K_s (a) and Korringa relation (b) in the normal state at 14 T.

Figure 4. ^{93}Nb spin-lattice relaxation rate T_1^{-1} in the superconducting state of the Nb$_3$Sn powder. (a) Relaxation rate ratio vs. temperature in 7 T, where R_s is the measured relaxation rate, and R_n is defined in the normal state as $(T/T_c)T_1^{-1}$ and in the superconducting state set equal to its value at T_c. The lines are guides to the eye. (b) BCS fit for the temperature dependence of the relaxation rates at 3.2 T and 7 T, shown separately. The fitting results are shown by curves giving $\Delta(0) = 2.7 \pm 0.3\,k_B T_c$ at 3.2 T and $\Delta(0) = 2.33 \pm 0.07\,k_B T_c$ at 7 T.

4.3. Superconducting state measurements

The spin lattice relaxation rate $R_s = T_1^{-1}$ was measured at the central transition in the superconducting state for both 3.2 T and 7 T. Figure 4(a) shows the 7 T data, which is normalized to the relaxation rate R_n at T_c, where $T_1 = 20.5$ ms. To better reflect the normal state behavior of T_1^{-1}, R_n is defined in the normal state as $(T/T_c)T_1^{-1}$ and in the superconducting state set equal to its value at T_c. The ratio R_s/R_n does not decrease immediately below T_c. This can be attributed to quasiparticle coherence; there is no evidence for a Hebel–Slichter peak [4]. The temperature dependence of R_s for the quasiparticle states at both 3.2 T and 7 T are fit to a modified BCS theory that accounts for strong-coupling effects. This is shown in figure 4(b) in the low temperature limit equation (6), with the superconducting energy gap $\Delta(T)$ phenomenologically expressed in equation (7) [8]. This equation comes from a fit to the theoretical BCS energy gap incorporating strong-coupling from the heat capacity jump $\Delta C/C$. The observed

exponential reduction of R_s is consistent with the appearance of an energy gap in the quasiparticle spectrum having the following form in the low temperature limit [4]:

$$T_1^{-1} \propto \exp\left(-\Delta(T)/k_B T\right) \qquad (6)$$

$$\Delta(T) = \Delta(0)\tanh\left\{\frac{\pi k_B T_c}{\Delta(0)}\left[\frac{2}{3}\left(\frac{T_c}{T}-1\right)\frac{\Delta C}{C}\right]^{1/2}\right\}. \qquad (7)$$

In the above expression we take the heat capacity jump, $\Delta C/C$, from our heat capacity measurement. Then the energy gap $\Delta(0)$ is inferred to be $\Delta(0) = 2.7 \pm 0.3\,k_B T_c$ at 3.2 T and

$\Delta(0) = 2.33 \pm 0.07 \, k_\mathrm{B} T_\mathrm{c}$ at 7 T, indicating magnetic field suppression of the order parameter. This suppression behavior is also seen in V_3Si from STM measurements [9]. A previous report on Nb_3Sn in zero field from tunneling measurements [10], gives $\Delta(0) = 2.1 \, k_\mathrm{B} T_\mathrm{c}$, while another report from heat capacity measurements [11], gives $\Delta(0) = 2.45 \, k_\mathrm{B} T_\mathrm{c}$. Both of them are larger than $\Delta(0) = 1.764 \, k_\mathrm{B} T_\mathrm{c}$ for weak-coupling BCS superconductivity, indicating strong-coupling behavior.

Following excitation from the NMR pulse, the energy relaxation of the ^{93}Nb nuclei is determined by the average of rates over all electronic quantum states constrained by the superconducting energy gap $\Delta(T)$. Following equation (6), extrapolation of the gap value to the zero field limit, leads to a result higher in value than other work referenced above. We note that in figure 1(a) there are satellite contributions overlapping with the central transition, meaning that the satellite relaxation might affect our T_1 measurement. However, we measured T_1 at the first satellite finding that the difference between T_1 at the central transition and at the satellite is within experimental error. Consequently, the satellite contribution is not an explanation. Similarly, we have also excluded the possibility of contributions from vortex dynamics by measuring the spin-spin relaxation rate T_2^{-1} as a function of magnetic field. This work will be presented separately. Nonetheless, T_1 is necessarily an average including the possibility of sub-gap electronic states, which might be an explanation for these differences. Alternatively, the Nb_3Sn band structure is expected to be complex. Consequently the gap average over different crystal orientations might also play a role.

5. Conclusion

In summary, a high-quality Nb_3Sn powder sample with cubic structure was investigated by nuclear magnetic resonance. Anisotropy in the Knight shift was found from measurement and analysis of the ^{93}Nb NMR spectrum. It was also found that under certain temperature and field conditions, highly crystalline powder grains can be aligned.

The Knight shift and T_1^{-1} in the normal state were measured. The decrease of Knight shift on cooling indicates that core polarization is enhanced at lower temperatures. In the superconducting state, the measurement of the spin-lattice relaxation rate, T_1^{-1}, is compared to BCS theory, giving an energy gap $\Delta(0) = 2.7 \pm 0.3 \, k_\mathrm{B} T_\mathrm{c}$ at 3.2 T and $\Delta(0) = 2.33 \pm 0.07 \, k_\mathrm{B} T_\mathrm{c}$ at 7 T, indicating suppression of the order parameter by magnetic field. In addition, quasiparticle coherence effects are observed near T_c in 7 T, in absence of a Hebel–Slichter peak.

Data availability statement

All data that support the findings of this study are included within the article (and any supplementary files).

ORCID iDs

Gan Zhai ⓘ https://orcid.org/0000-0001-6623-9565
Zuhawn Sung ⓘ https://orcid.org/0000-0002-5927-1775
Chiara Tarantini ⓘ https://orcid.org/0000-0002-3314-5906
David C Larbalestier ⓘ https://orcid.org/0000-0001-7098-7208

References

[1] Zhou J 2011 *The Effects of Variable Tin Content on the Properties of A15 Superconducting Niobium-3-Tin* (The Florida State University)
[2] Devred A, Backbier I, Bessette D, Bevillard G, Gardner M, Jong C, Lillaz F, Mitchell N, Romano G and Vostner A 2014 *Supercond. Sci. Technol.* **27** 044001
[3] Posen S, Lee J, Seidman D N, Romanenko A, Tennis B, Melnychuk O S and Sergatskov D A 2021 *Supercond. Sci. Technol.* **34** 025007
[4] McLaughlin D 1976 *Solid State Physics* (Academic)
[5] Mitrović V, Sigmund E, Eschrig M, Bachman H, Halperin W P, Reyes A, Kuhns P and Moulton W 2001 *Nature* **413** 501
[6] Fradin F Y and Zamir D 1973 *Phys. Rev.* B **7** 4861
[7] Carter G Bennett L and Kahan D 1977 *Metallic Shifts in NMR: A Review of the Theory and Comprehensive Critical Data Compilation of Metallic Materials* (Pergamon)
[8] Halperin W and Varoquaux E 1990 *Helium Three* (*Modern Problems in Condensed Matter Sciences* vol 26) ed W Halperin and L Pitaevskii (Elsevier) pp 353–522
[9] Ding S, Zhao D, Jiang T, Wang H, Feng D and Zhang T 2023 *Quantum Front.* **2** 3
[10] Orlando T P, McNiff E J, Foner S and Beasley M R 1979 *Phys. Rev.* B **19** 4545
[11] Junod A, Jarlborg T and Muller J 1983 *Phys. Rev.* B **27** 1568